

Industrial extrusion and characterisation of alloy AA2013

A.J. den Bakker¹, T. Minoda², L. 't Hoen-Velterop³

¹Nedal Aluminium B.V., Utrecht, The Netherlands

²Sumitomo Light Metal Industries Ltd, Tokyo, Japan

³NLR, Amsterdam, The Netherlands

Although originally developed as an alternative to AA2024 for aerospace applications, the enhanced workability and promising product characteristics of alloy AA2013 present an interesting proposition for applications in other markets. To assess the characteristics of AA2013, industrial extrusion trials were conducted. It was found that the alloy has favourable processing characteristics. The mechanical properties following press quenching and artificial aging were comparable of those for AA2024. Fine tuning of the processing conditions is however required to achieve optimised product quality.

Keywords: AA2013, Extrusion Processing, Properties

1. Introduction

In many structural aerospace applications the AA2024 aluminium alloy has been the material of choice for more than a half century, due to its high strength and excellent fatigue resistance. Nevertheless, precautions have to be taken to prevent corrosion-related issues, through the application of a clad layer or by anodising. Also the relatively poor formability of the alloy limits the range of product shapes and the minimal attainable wall thickness in extrusion processing.

Recently, Sumitomo Light Metals developed the alloy AA2013 for use in the aerospace sector[1]. Based on the Al-Mg-Si group, Cu is added to achieve increased strength. As the extrudability is relatively insensitive to Cu additions, the superior workability of the Al-Mg-Si alloys group is only slightly impaired. Due to this favourable workability, hollow extrusions produced by means of porthole dies are possible, thus widening the geometrical product range to complex, multi-hollow shapes. Furthermore, based on the reduced alloy content, it is expected that good mechanical properties can be achieved through press-quenching extruded shapes directly after extrusion instead of a more elaborate, cost increasing, separate solution heat treatment procedure. Based on these features, an evaluation programme was initiated to assess the suitability of the developed alloy for processing on regular extrusion presses into complex shapes, as a substitute for the relatively difficult to extrude 7xxx series aluminium alloys, such as AA7020.

2. Experimental programme

In the experimental programme the hot deformation characteristics of the alloy are determined through laboratory-scale compression tests, whilst the processing performance coupled to product characteristics was determined through industrial extrusion trials. For these tests 203 mm diameter industrial DC cast and homogenised billets of 1000 mm length were produced by Sumitomo Light Metals. The composition range is shown in Table 1. Images depicting the typical, fine-grained microstructure are presented in Fig. 1.

Table 1 Alloy composition range for AA2013 (values in mass%)

Element	Si	Fe	Cu	Mn	Mg	Cr	Zn	Ti	Others, each	Others, total
min	0.6	---	1.5	---	0.8	0.04	---	---	---	---
max	1.0	0.40	2.0	0.25	1.2	0.35	0.25	0.25	0.05	0.15

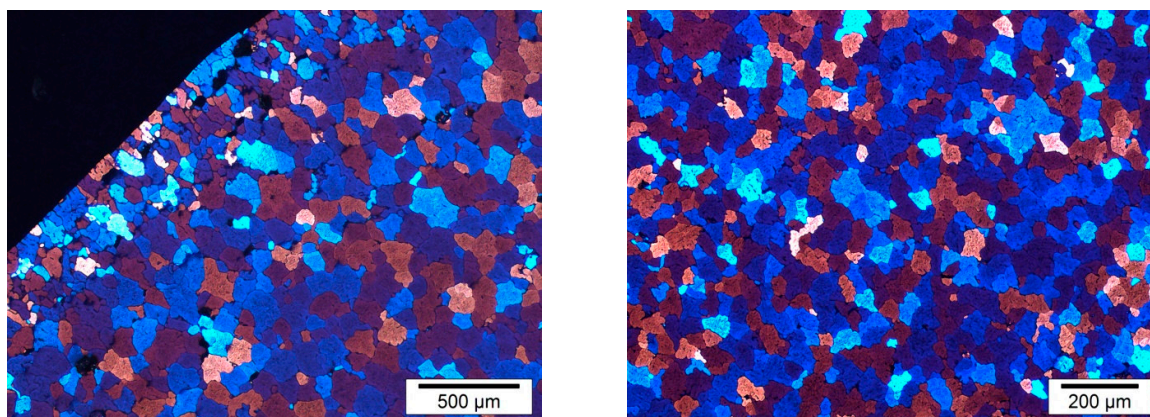


Figure 1 Grain structure of the billet material.
Left : edge section of the billet, right: centre area

2.1 Flow stress

One of the major factors influencing the extrudability of a material is the ease of deformation, typified by its constitutive behaviour, where the flow stress is expressed as a function of strain, strain rate and temperature. The flow stress of the alloy AA2013, in comparison to alloy AA7020 was determined by means of compression tests [2]. Using the set-up shown in Fig. 2, open die forging tests are performed, where the material flows askew to the tool motion due to the uniaxially applied strain. The specimens have a diameter of 11 mm and an initial height of 18 mm. The crucible guides the upsetting tools and secures a constant surrounding temperature. The friction between the tools and the specimen is minimised by the use of PTFE foils between the tool and the specimen. Tests were performed with strain rates ranging from 1 s^{-1} to 50 s^{-1} at temperatures of 450°C and 500°C . In the tests the flow stress vs. strain was recorded up to a strain of approximately 0.9.

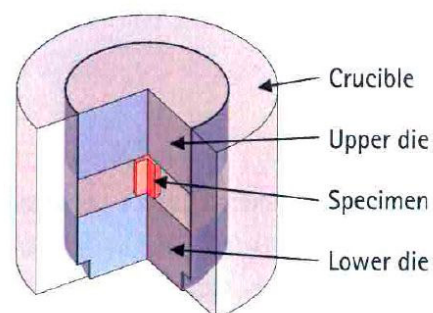


Figure 2 Forging test set-up

2.2 Extrusion trials

The extrusion trials were performed on a 25MN direct extrusion press at Nedal Aluminium. Apart from a 25 mm diameter rod which is further not discussed in this paper, two types of extrusions were produced (Fig. 3): profile A, a rectangular box-section extrusion and profile B, a single-hollow extrusion used for commercial applications. Both sections were produced with porthole dies.

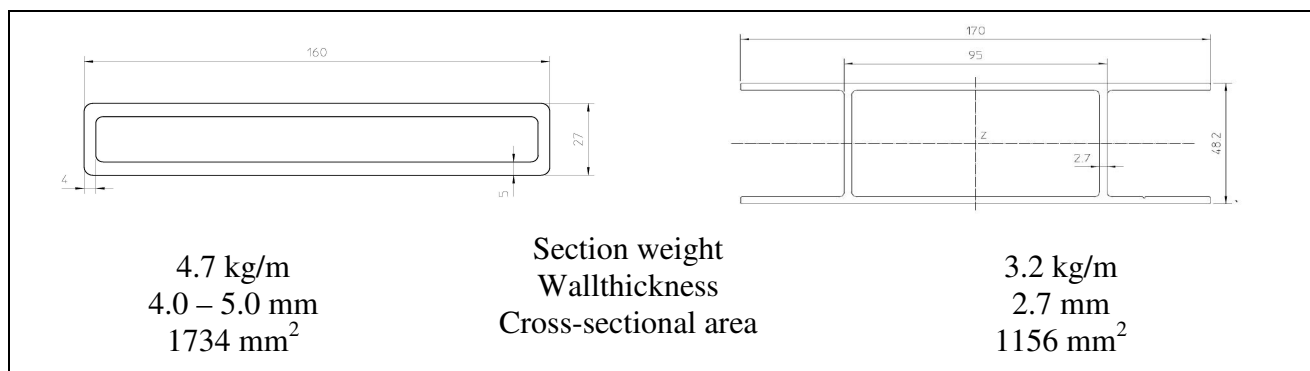


Figure 3 Cross-section geometry of extruded shapes (left: profile A ; right: profile B)

The billets were pre-heated in a gas-fired billet furnace to the set-point temperature. For each profile five billets were extruded. Profile A was press quenched by means of water sprays in the cooling tunnel; profile B was fully air quenched. Following the extrusion of each billet the discard of each billet (the butt-end) was sheared and the next billet was loaded into the container and extruded onto the filled die. The billet-to-billet transition caused by this process was cut from the extruded length and discarded. The extruded lengths were stretched and subsequently cut into lengths of 6000 mm for further processing. From representative parts originating from approximately the middle of an extruded length, samples were cut for aging tests. Aging was performed in a laboratory furnace at 160°C, 190°C and 220°C for aging times ranging from 1 hour up to 24 hours (after a storage time at room temperature of 1 month) in order to determine the optimal aging procedure. The aged samples were characterised by means of tensile testing on a 100 kN tensile test machine. After establishing the optimal aging parameters the remaining samples lengths were heat treated to the peak aged condition (i.e., T5 temper).

2.3 Fatigue testing

Three S/N curves were determined, in longitudinal and transverse direction for profile A and in transverse direction for profile B. The specimens in the longitudinal direction contained no weld seam while the specimens in the transverse direction did contain a weld seam roughly centered in the gauge length of the specimen. For each S/N curve 20 specimens were machined according to the drawing in Fig. 4. The surfaces of the specimens were milled to remove the extrusion surface that, for profile A, contained small cracks perpendicular to the longitudinal direction. The specimen surfaces and sides were polished in the gauge section to remove all machining marks that might induce fatigue crack initiation.

Ambient temperature constant amplitude fatigue testing was performed in accordance with ASTM E466-96 in a 100 kN Amsler Vibrophore high frequency resonance machine at a stress ratio $R = S_{min}/S_{max}$ of 0.1. The test frequency was 67 Hz for profile A and 75 Hz for the thinner profile B. Each test was stopped after failure of the specimen or after reaching 10^7 cycles, which was assumed to be the fatigue limit. At least three specimens were tested per load level to obtain insight in the spread in fatigue life.

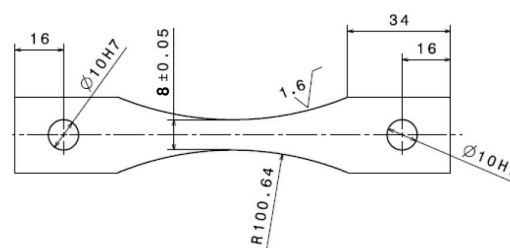


Figure 4 Geometry of the fatigue specimens

3. Results and Discussion

3.1 Flow stress

The results of the determination of the flow stress are presented in Fig. 5. The flow stress curves for the different combinations of temperature and strain rate for AA2013 are presented, together with a scales comparison with AA7020. The data for alloy AA7020 is determined in the same set-up and at equivalent settings as for AA2013. The scaled flow stress values in comparison with AA7020 are shown for a strain value of 0.5. At low strain rates the flow stress is independent of the strain, with somewhat higher values for the lower test temperature. At high strain rates the flow stress initially increases but subsequently gradually decreases with increasing strain. In comparison with AA7020 the flow stress of AA2013 is approximately 5-15% lower, depending on specific conditions. Further tests were attempted at 550°C, however during upsetting of the AA2013 alloy the samples fractured into several smaller parts. This was caused by local incipient melting within the sample, causing loss of structural integrity of the sample.

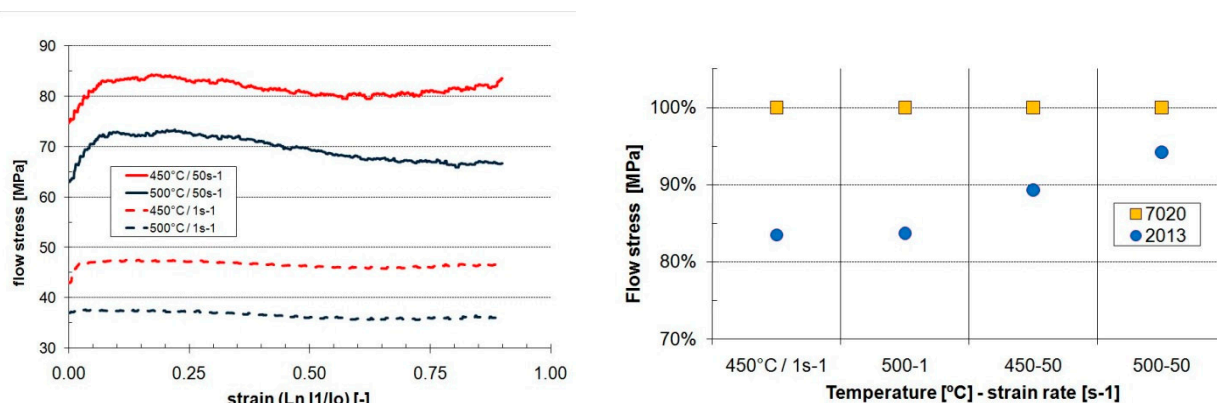


Figure 5 Flow stress curves for AA2013 (left) and flow stress relative to AA7020 (right)

3.2 Extrusion

Extrusion processing was performed without any irregularities. All investigated shapes exhibited regular appearance, with a visual surface quality similar to regular 6xxx alloy extrusions. In Table 3 a comparison is shown for the required extrusion pressure (at similar extrusion speeds and billet lengths) for AA7020 and AA2013 for profile B. Despite the lower billet temperature (which will increase the flow stress, as shown in the previous section), the breakthrough pressure (i.e. the pressure required to initiate flow of the metal through the die) for alloy AA2013 is lower than the breakthrough pressure for AA7020. The same holds for the pressure at the end of the extrusion cycle, although the difference in this case is somewhat larger. Therefore the trend which is observed for the flow stress as determined by the forging tests is reflected in the extrusion tests.

Table 3 Extrusion data for profile B

Alloy	Billet temperature [°C]	Start pressure [Bar]	Final Pressure [Bar]
AA7020	510	283	168
AA2013	480	275	145

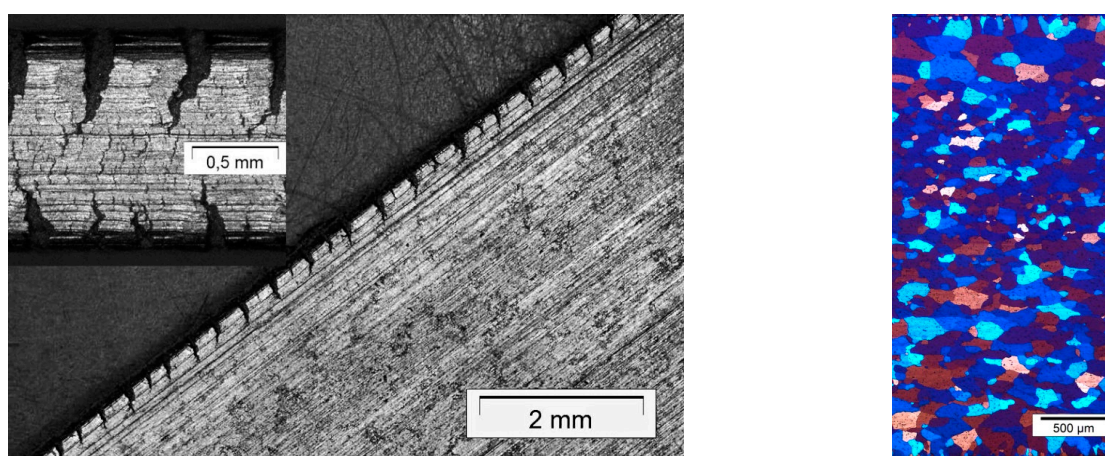


Figure 6 Degradation of the edge of the extrusion of profile B (left) and grain size over wall thickness in transverse direction of profile A (right)

During the test the extrusion speed was increased to assess the extrudability. This resulted in degradation of the edges during the extrusion of profile B (Fig. 6) and ultimately hot tearing of the extrusion surface. Considering the relatively low billet temperature, it is concluded that within the

investigated parameter range, the extrudability of alloy AA2013 is limited by the lower melting temperature phases instead of the flow stress.

In Fig. 6 a typical representation of the microstructure of profile A is presented. The structure is a fully recrystallised with a small gradient in grain size over the thickness of the extrusion. Despite the fact that this micrograph originates from the location of the weld seam, this is not evident from the microstructure. Therefore it is concluded that due to complete recrystallisation the original weld line has been eradicated as a microstructural feature and a continuous microstructure is achieved.

3.3 Static mechanical properties

The typical mechanical properties for the extrusions after aging to peak strength values (according to an aging cycle determined through aging tests) are presented in Table 4 for the longitudinal direction and Table 5 for the transverse direction. The extrusion which was water quenched after extrusion, profile A, has a somewhat higher yield stress, however the ultimate tensile strength is lower than the air quenched profile B. The properties compare well with the values reported by Minoda et.al. [1] The slightly lower values for the yield stress may well be explained by the different processing route, i.e. the extrusions are press-quenched instead of undergoing a full T6511 heat treatment. Nevertheless, the extrusion test has demonstrated that excellent mechanical properties can be achieved through a cost-efficient extrusion process.

Table 4 Mechanical properties in peak aged condition - longitudinal direction

Profile	Yield strength [MPa]	UTS [MPa]	Elongation (A5) [%]
Profile A (water quenched)	340-350	365-385	8-10
Profile B (air quenched)	325-340	380-400	9-12
AA2013 T6511	365	400	14

Table 5 Mechanical properties in peak aged condition - transverse direction

Profile	Yield strength [MPa]	UTS [MPa]	Elongation (A5) [%]
Profile A (water quenched)	278	363	9.5
Profile B (air quenched)	286	361	10

3.4 Fatigue properties

The S/N curve data are shown in Fig. 7 for profile A in both orientations and in the transverse (LT) orientation for profile B, together with reference data from other sources. Profile A showed a higher fatigue strength and smaller spread in fatigue life for the transverse direction than for the longitudinal direction. The spread in fatigue life in transverse direction was similar for both profiles, but the profile A had a higher fatigue strength. The fatigue strengths of profile A in longitudinal direction and of profile B in transverse direction are similar.

The fracture surfaces of both longitudinal and transverse specimens from profile A showed similar appearances, revealing no indications of the weld seam. This is in agreement with the microstructure shown in figure 7, where the weld seam cannot be recognised in the microstructure.

It can be seen that the fatigue properties of the present extrusions are a bit lower than those reported in reference 1. The fatigue life at higher stresses is lower while the fatigue strength at 10^7 cycles is similar to the one reported for R=0.02 and only slightly lower than the one reported for R=0.3.

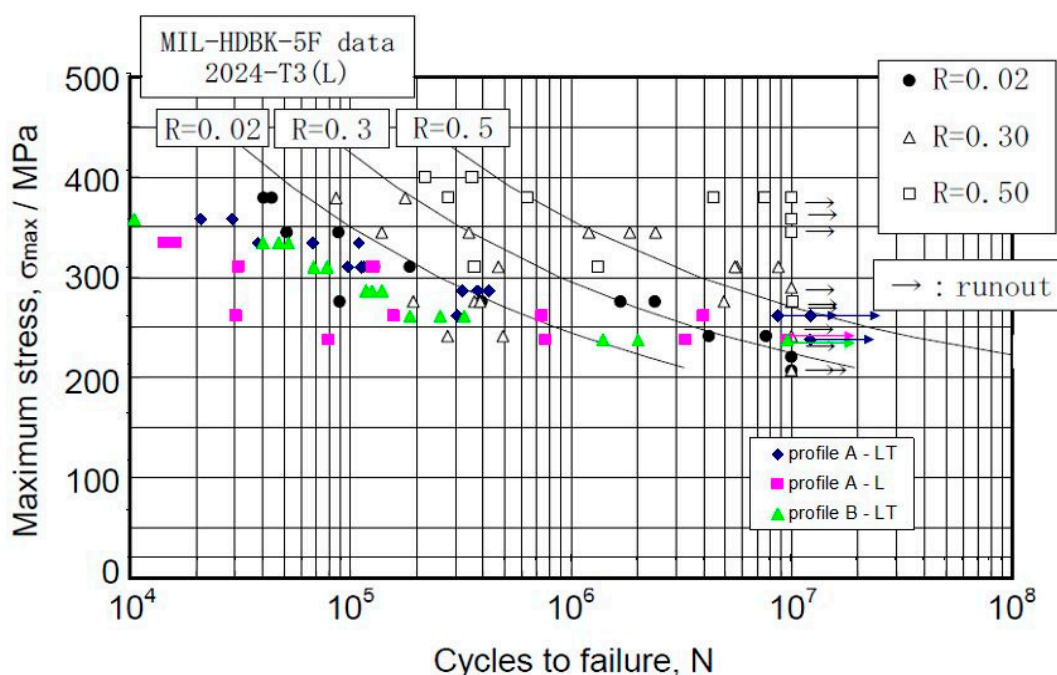


Figure 7 Constant amplitude fatigue test results at $R = 0.1$ (L indicates testing in longitudinal direction and LT indicates testing in transverse direction). The data is superimposed on values from Minoda et.al. [1] and data for AA2024 T3 from [3]

4. Conclusion

The alloy AA2013 was initially developed as an alternative to AA2024, aiming at improved production characteristics. Through an experimental programme the performance of the alloy AA2013 was assessed for industrial extrusion processing into products outside the aerospace markets. It was found that the extrudability of the alloy compares favourably to AA7020 and that relatively complex hollow shapes can be produced utilising porthole dies. Moreover, it was shown that good mechanical properties can still be achieved if the alloy is press-quenched and artificially aged instead of applying a separate solution heat treatment. It is expected that the observed hot tearing can be avoided by further fine-tuning of the extrusion process and thus further improving the productivity of the alloy .

5. Acknowledgements

This research was partly carried out under the project number MA.07066 in the framework of the Research Program of the Materials innovation institute M2i.

References

- [1] T. Minoda, K. Kato, H. Sano and Y. Yoshida: Aluminium 2000 6th World Congress, Florence, It. (2007).
- [2] IFUM Flow stress determination of alloy AA2013, Hannover (2009)
- [3] Anon. Military handbook : Metallic materials and elements for aerospace vehicle structures, (1998)